Emission quenching induced by intervalence charge transfer in Pr^{3+}- or Tb^{3+}-doped $YNbO_4$ and $CaNb_2O_6$

2007 J. Phys.: Condens. Matter 19 386230

(http://iopscience.iop.org/0953-8984/19/38/386230)

J. Phys.: Condens. Matter **19** (2007) 386230 (11pp) doi:10.1088/0953-8984/19/38/386230

Emission quenching induced by intervalence charge transfer in Pr^{3+}- or Tb^{3+}-doped $YNbO_4$ and $CaNb_2O_6$

P Boutinaud[1], **E Cavalli**[2] **and M Bettinelli**[3]

[1] Laboratoire des Matériaux Inorganiques—UMR 6002, Université Blaise-Pascal et ENSCCF, Aubière, France
[2] Dipartimento di Chimica Generale ed Inorganica, Chimica Analitica, Chimica Fisica, Università di Parma, Parma, Italy
[3] Dipartimento Scientifico e Tecnologico, Università di Verona, and INSTM, UdR Verona, Verona, Italy

E-mail: Philippe.Boutinaud@univ-bpclermont.fr

Received 18 July 2007, in final form 10 August 2007
Published 4 September 2007
Online at stacks.iop.org/JPhysCM/19/386230

Abstract

The excitation and emission properties of Pr^{3+} and Tb^{3+} ions doped into $YNbO_4$ (hereafter YNB) and $CaNb_2O_6$ (hereafter CNB) have been studied as a function of the temperature in the 10–600 K range. The observed quenching of the luminescence from the $^3P_0$ (Pr^{3+}) and $^5D_3$ (Tb^{3+}) states has been related to an electron transfer process from the trivalent rare earth to the Nb^{5+} ion inducing the formation of an intervalence charge transfer (IVCT) state. On this basis a detailed picture of the excited-state dynamics of the investigated compounds is presented, taking into account the characteristics of the host lattices and of the involved optically active ions.

1. Introduction

The quenching of the Pr^{3+} blue emission by crossover to a low-lying intervalence charge transfer state (IVCT) can be conveniently exploited in the realization of efficient red-emitting phosphors. It has recently been investigated in a number of mixed oxides like titanates, vanadates, niobates and tantalates [1–3] as a follow-up to studies by Reut and Ryskin [4] and Blasse and Bril [5] carried out in the 1970s. An IVCT state originates from the transfer of an electron from the Pr^{3+} weakly reducing ion to the d^0 transition metal ion constituting the host lattice, and its presence is revealed in the excitation spectrum of the Pr^{3+} luminescence by an extra band located in the 25 000–35 000 cm^{-1} range. Such a behaviour is consistent with the relatively high optical electronegativities ($\chi_{opt}(M^{n+})$) of the d^0 metal cations M^{n+} = Ti^{4+}, V^{5+}, Nb^{5+}, etc, and with the natural tendency of the Pr^{3+} ion to be oxidized to the tetravalent state, evidenced by the low value of the optical electronegativity of Pr^{4+} [6]. Depending on its energy position, the IVCT state plays an active role in the dynamics of the excited states of Pr^{3+} mostly providing an efficient quenching channel for the $^3P_0$ and in some cases also for the $^1D_2$ emission [2, 3]. On this basis, it has been possible to formulate

a preliminary criterion to predict in which crystals the $^3P_0$ emission is completely quenched at room temperature but the red $^1D_2$ emission is not [2, 3]. These studies have also been extended to the case of the Tb^{3+} ion which has a comparable redox behaviour to Pr^{3+}, as evidenced by the relative variation in the binding energy of the 4f electrons for trivalent lanthanides [7]. Recently it has been shown that the green $^5D_4 \rightarrow {}^7F_5$ emission of Tb^{3+} is completely quenched at room temperature by the IVCT process in YVO_4 and $CaTiO_3$, only partially quenched in $LaVO_4$, $YNbO_4$ and $YTaO_4$ and not quenched at all in YPO_4 [8]. Despite the extensive work carried out in the recent past, there still are different classes of crystal for which the information is largely incomplete: niobates, molybdates, etc. In this paper we have focused our attention on two niobate host lattices having different crystal structures, i.e. $YNbO_4$ and $CaNb_2O_6$. We have carried out a comparative investigation in order to evidence the influence of IVCT on the excited-state dynamics of the Pr^{3+} and Tb^{3+} ions in these materials, in the light of their structural dissimilarities and of the different spectroscopy of the undoped hosts.

2. Experimental details

2.1. Synthesis and structural data

Pure and 0.5% Pr^{3+}- or Tb^{3+}-doped YNB and CNB crystalline powders were prepared by solid state reactions using conventional techniques. All samples were checked to be single phase by x-ray powder diffraction. YNB (fergusonite) belongs to the monoclinic $C2/c$ space group, with cell parameters $a = 7.645$ Å, $b = 10.999$ Å, $c = 5.317$ Å, $\beta = 138.4°$ [9]. Its structure consists of isolated NbO_4 distorted tetrahedra and of Y^{3+} ions located in eight-fold cavities having distorted square antiprismatic geometry. The average Y–O interatomic distance is 2.36 Å. CNB has a columbite structure belonging to the orthorhombic $Pbcn$ space group, with cell parameters $a = 14.926$ Å, $b = 5.752$ Å, $c = 5.204$ Å [10]. It can be described as a network of NbO_6 octahedra sharing edges with two other ones to form chains running along the c axis. The Ca^{2+} ions are surrounded by eight oxygen atoms in a very distorted cubic geometry. The average Ca–O interatomic distance is 2.47 Å. The trivalent doping ions replace Y^{3+} or Ca^{2+}. In the latter case charge compensation mechanisms are active and contribute to the inhomogeneous broadening of the spectral features. The average Nb^{5+}–O^{2-} distances are respectively 1.89 Å in YNB and 2.02 Å in CNB.

2.2. Spectroscopic measurements

The photoluminescence spectra were measured in the 10–600 K temperature range using a Triax 550 monochromator equipped with a nitrogen-cooled CCD camera and a R928 Hamamatsu photomultiplier (Jobin-Yvon Symphony system). The excitation light was selected from a xenon lamp using a Triax 180 monochromator. The spectra in the 10–300 K range were obtained by cooling the samples by means of a He closed cycle cryostat (Air Products Displex DE-202), and those in the 300–600 K range with the help of a home-made copper holder heated by a thermocoax wire connected to a Thermolyne regulator. The temporal decay profiles were recorded at room temperature upon nitrogen laser excitation (337 nm) using an HR1000 Jobin-Yvon monochromator and a 400 MHz Lecroy digital oscilloscope with 50 Ω input impedance.

3. Experimental results

3.1. Luminescence spectra and role of the IVCT

A selection of continuous wave emission spectra of Pr^{3+} and Tb^{3+} ions in YNB and CNB is presented in figure 1 upon various excitation wavelengths at 270 nm (niobate excitation),

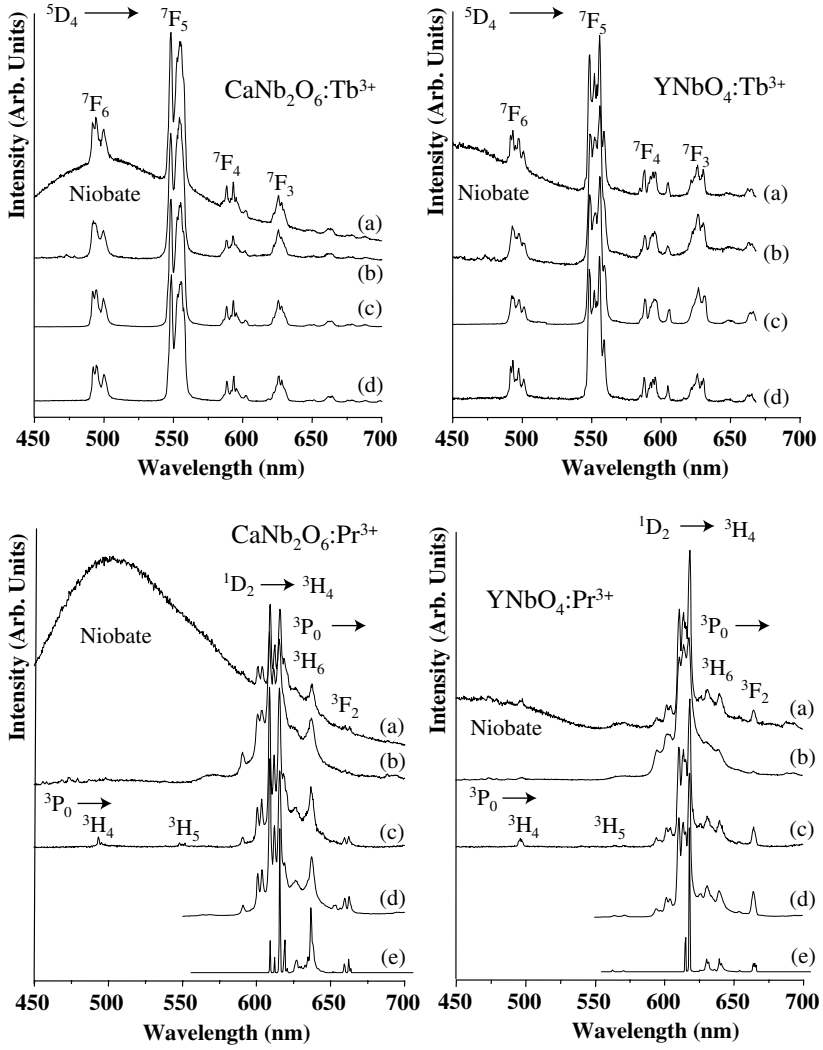

Figure 1. Steady state emission spectra of Pr^{3+} or Tb^{3+}-doped $CaNb_2O_6$ and $YNbO_4$ at different temperatures and for different excitation wavelengths. 'Niobate' indicates the niobate group emission. For $CaNb_2O_6$:Tb^{3+} and $YNbO_4$:Tb^{3+}: Exc = 270 nm, T = 295 K (a), Exc = 270 nm, T = 481 K (b), Exc = 320 nm, T = 295 K (c), Exc = 375 nm, T = 295 K (d); for $CaNb_2O_6$:Pr^{3+} and $YNbO_4$:Pr^{3+}: Exc = 270 nm, T = 293 K (a), Exc = 270 nm, T = 490 K (b), Exc = 320 nm, T = 293 K (c), Exc = 440 nm, T = 293 K (d), Exc = 440 nm, T = 10 K (e).

320 nm (IVCT excitation, see below), 375 nm (Tb^{3+} $^7F_6 \rightarrow {}^5D_3$) or 440 nm ($Pr^{3+}$ $^3H_4 \rightarrow {}^3P_2$).

At room temperature and above it the Tb^{3+} luminescence in both niobates consists of $^5D_4 \rightarrow {}^7F_J$ (J = 6–3) emission lines. No $^5D_3$ emission is present, independently of the excitation conditions. The broad luminescence bands occurring in the room-temperature spectra upon 270 nm excitation are ascribed to the emissions of the NbO_4^{3-} and NbO_6^{7-} units, in agreement with the spectra of pure YNB and CNB shown in figure 2 and with literature data [11, 12].

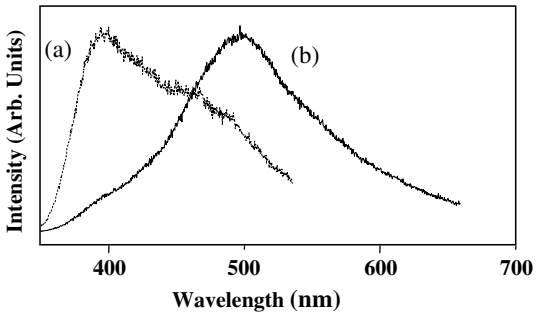

Figure 2. Steady state emission spectra of undoped $YNbO_4$ (a) and $CaNb_2O_6$ (b) at room temperature upon 275 nm excitation.

Their presence indicates that the energy transfer from the host to Tb^{3+} is relatively inefficient, at least at 298 K. It is also conceivable that other states (probably the IVCT) more or less efficiently absorb the 270 nm radiation. The niobate emission is almost completely quenched at about 500 K. Similarly, the luminescence of the Pr^{3+}-doped samples is composed mainly of the red $^1D_2 \rightarrow {}^3H_4$ emission. Weak contributions from the $^3P_0$ level are observed in the bluish-green ($^3P_0 \rightarrow {}^3H_4$), green ($^3P_0 \rightarrow {}^3H_5$) and red ($^3P_0 \rightarrow {}^3H_6$ and $^3P_0 \rightarrow {}^3F_2$) spectral regions. The $^1D_2 \rightarrow {}^3H_4$ and $^3P_0 \rightarrow {}^3H_6$ overlapping transitions can be separated only in the low-temperature spectra, in which the thermally activated processes are nearly absent. The 10 K spectra shown in figure 1 confirm the prevalence of the emission from $^1D_2$ and the significant quenching of that from $^3P_0$. This quenching slightly depends on the pumping conditions: for example, the intensity of the $^3P_0 \rightarrow {}^3F_2$ signal is somewhat higher when observed upon 440 nm than upon 320 nm excitation. Such a behaviour can be accounted for by invoking the 'virtual recharge' model and considering that the direct pumping in the IVCT contributes to by-passing the population of $^3P_0$ level [3]. The low-temperature emission spectra of the Tb^{3+}-doped niobates excited at 365 nm ($^7F_6 \rightarrow {}^5D_3$) or 300 nm (IVCT) are presented in figures 3(a) and (b) respectively. The $^5D_3$ emission appears only upon excitation at 365 nm. It is strong in CNB:Tb^{3+} and weak in YNB:Tb^{3+}. The absence of $^5D_3$ emission under pumping at 300 nm suggests that the population of this level is by-passed upon direct excitation in the IVCT band, similarly to the case of Pr^{3+}-doped niobates. The room-temperature decay profiles of $^1D_2 \rightarrow {}^3H_4$ (Pr^{3+}) and $^5D_4 \rightarrow {}^7F_5$ (Tb^{3+}) emission signals are exponential, with time constants in the range 40–60 μs for $^1D_2$ emission and around 600 μs for $^5D_4$ emission (550 μs for YNB and 670 μs for CNB).

3.2. Excitation spectra and host sensitization

The room- and high-temperature excitation spectra of the red $^1D_2$ (Pr^{3+}) and green $^5D_4$ (Tb^{3+}) emissions are shown in figure 4.

At 298 K they are dominated by broad bands peaking in the 32 000–33 000 cm^{-1} range (≈312–300 nm), that we ascribe to IVCTs on the basis of previous works [1, 3, 8]. These bands present components on their high-energy sides at about 36 300 cm^{-1} (≈275 nm). These features are assigned to niobate absorptions, being nearly coincident with the transitions observed in the excitation spectra of the undoped hosts (figures 4(e) and (f)). On passing to the high-temperature spectra, the relative intensity of the niobate absorption of YNB significantly increases with respect to that of the IVCT band, suggesting a temperature-assisted

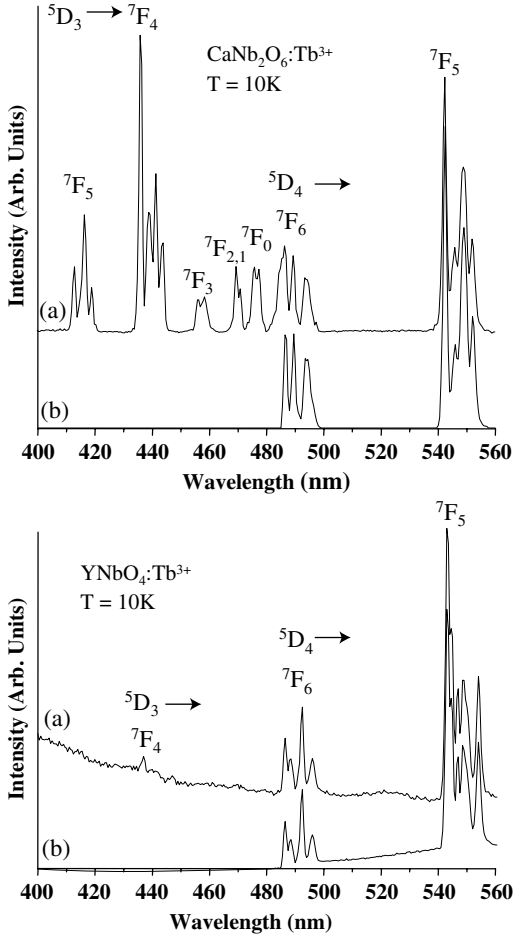

Figure 3. Emission spectra at low temperature of Tb^{3+}-doped $CaNb_2O_6$ and $YNbO_4$. (a): Exc = 365 nm, (b): Exc = 300 nm.

host sensitization of both Pr^{3+} and Tb^{3+} emissions in this host. The comparison between the temperature dependences of the integrated emission intensities of the niobate, $^1D_2 \rightarrow {}^3H_4$ (Pr^{3+}) and $^5D_4 \rightarrow {}^7F_5$ (Tb^{3+}) transitions, shown in figure 5, is fully consistent with this process.

In the case of YNB in fact the temperature quenching of the host emission is associated to the increase of the Pr^{3+} or Tb^{3+} luminescence. The maximum emission intensity is at around 500 K in the Pr^{3+} case and at around 425 K in the Tb^{3+} case. Above these temperatures, a strong quenching of the lanthanide luminescence occurs. For CNB the situation is the opposite with respect to YNB: the niobate excitation signal is more intense at room temperature instead of at high temperature (figure 4). According to figure 5, the temperature quenching of the niobate luminescence in CNB:Tb^{3+} and CNB:Pr^{3+} is not associated with an increase of the rare earth emission, suggesting that no important host sensitization occurs in these compounds. The niobate bands present in the spectra of CNB:Tb^{3+} and CNB:Pr^{3+} in figure 4 then arise mainly from the direct excitation of the broad emission of the NbO_6^{7-} ion extending up to 700 nm.

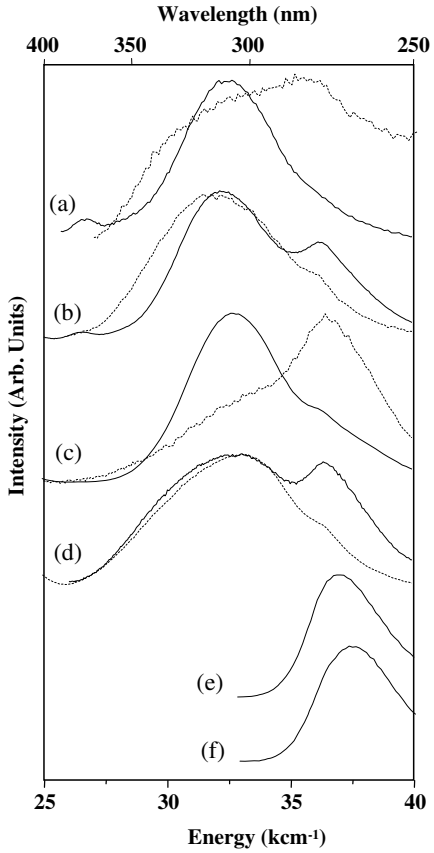

Figure 4. Excitation spectra of (a) $YNbO_4$:Tb^{3+} at $T = 295$ K (——) and $T = 511$ K (· · · · · ·), (b) $CaNb_2O_6$:Tb^{3+} at $T = 295$ K (——) and $T = 493$ (· · · · · ·), (c) $YNbO_4$:Pr^{3+} at $T = 295$ K (——) and $T = 473$ K (· · · · · ·), (d) $CaNb_2O_6$:Pr^{3+} at $T = 295$ K (——) and $T = 533$ K (· · · · · ·), (e) $CaNb_2O_6$ at $T = 298$ K, (f) $YNbO_4$ at $T = 298$ K. Observation wavelengths: 620 nm ((a)–(d)), 550 nm (e) and 500 (f).

3.3. Temperature behaviour of the emission and crossover to quenching states

The integrated intensity of the $^5D_4 \rightarrow {}^7F_5$ emission of Tb^{3+} in YNB and CNB was measured in the 300–600 K temperature range upon excitation at 375 nm. The results are plotted in figure 6.

The data were reasonably well reproduced using the model introduced by Struck and Fonger in the case of crossover to Franck–Condon shifted states [13]. Following this model, the temperature dependence of the emission intensity $I(T)$ is described by

$$I(T)/I_0 = [1 + A\exp(-E/kT)]^{-1}, \tag{1}$$

where A is close to 10^7 and E is the activation energy from the $4f^n$ state to its crossover with the quenching state. Indicative values of energy barriers for $^5D_4$ level are respectively 4500 cm^{-1} in YNB and 6050 cm^{-1} in CNB. The quenching temperature (temperature at which the emission intensity starts to reduce) is roughly evaluated at 440 K in the case of YNB:Tb^{3+} and 480 K in that of CNB:Tb^{3+}. The intensities of both $^5D_4$ and $^5D_3$ emission signals of CNB:Tb^{3+} have been measured also in the 10–300 K temperature range (figure 6). While the $^5D_4$ emission intensity is constant, the $^5D_3$ signal reduces by two decades in the range 100–300 K. The

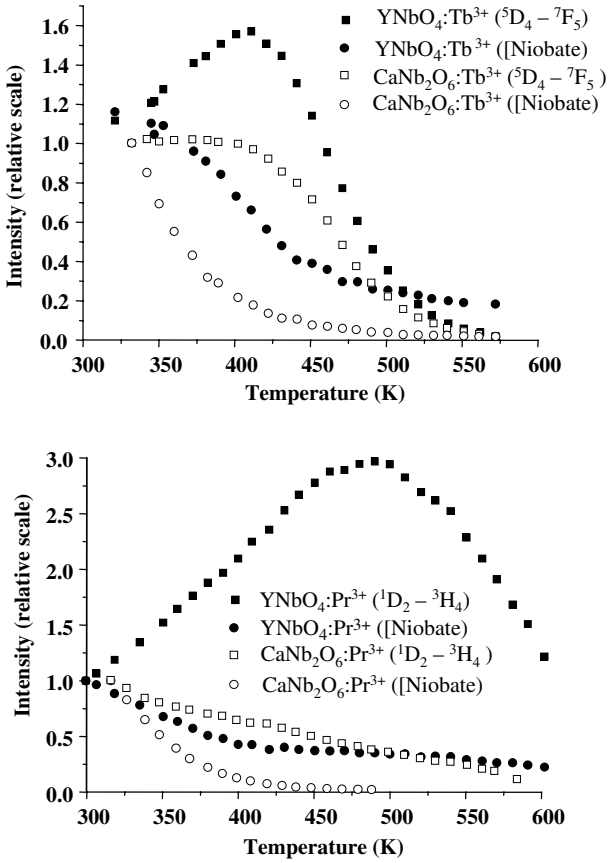

Figure 5. Temperature dependence of the green $^5D_4 \rightarrow {}^7F_5$, the red $^1D_2 \rightarrow {}^3H_4$ and of the niobate luminescence intensity in Tb^{3+}-doped and Pr^{3+}-doped niobates upon 270 nm excitation. The niobate group emission is indicated as 'Niobate'.

quenching temperature is about 100 K, and the activation energy for the crossover to the IVCT state has been estimated to be about 950 cm^{-1}.

The integrated intensities of the red $^1D_2 \rightarrow {}^3H_4$ and $^3P_0 \rightarrow {}^3F_2$ emissions of Pr^{3+} in YNB and CNB were measured in the temperature range 300–600 K upon 440 nm excitation. The results are very similar for both niobates, as shown in figure 7.

The data evidence a progressive quenching of the weak $^3P_0$ emission, whose intensity reduces of about 90% in the 300–500 K range, whereas that of the $^1D_2 \rightarrow {}^3H_4$ transition is nearly constant up to 500 K. The estimated quenching temperatures of the $^1D_2$ emission of Pr^{3+} are 530 K in CNB and 560 K in YNB. The crossover to the IVCT state, evaluated using equation (1), is located at 7150 cm^{-1} from the minimum of the $^1D_2$ level in CNB:Pr and at 7650 cm^{-1} in YNB:Pr. The thermal behaviour of the $^3P_0 \rightarrow {}^3F_2$ signal cannot be fitted using equation (1) because of the presence of other radiationless processes contributing to the depopulation of the emitting level. The most important is certainly the multiphonon relaxation [14, 15]: the maximum phonon energies of YNB and CNB are respectively ≈830 and ≈900 cm^{-1}, so not more than four phonons are required to bridge the energy gap between $^3P_0$ and $^1D_2$ (≈3500 cm^{-1}). It is interesting to point out that the thermal behaviour of the Pr^{3+} emission in the investigated niobates is substantially different

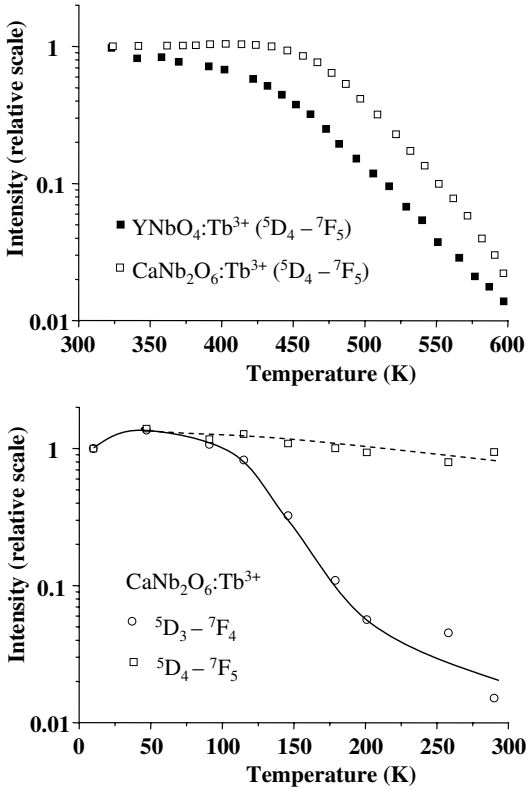

Figure 6. Temperature dependence of the green $^5D_4 \rightarrow {}^7F_5$ and blue $^5D_3 \rightarrow {}^7F_4$ luminescence intensity in the Tb^{3+}-doped niobates upon excitation in $^5D_3$ level. Solid and broken lines are guides for the eye.

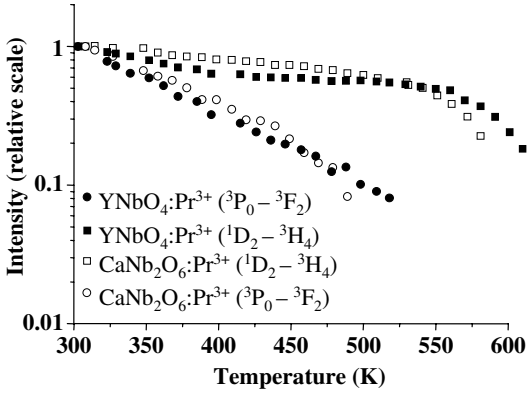

Figure 7. Temperature dependence of the red $^1D_2 \rightarrow {}^3H_4$ and $^3P_0 \rightarrow {}^3F_2$ luminescence intensity in Pr^{3+}-doped niobates upon excitation in $^3P_2$ level (440 nm).

from that in titanates ($CaTiO_3:Pr^{3+}$) or vanadates ($YVO_4:Pr^{3+}$), both showing complete quenching of the $^3P_0$ emission at room temperature and strong $^1D_2$ emission quenching in the temperature range 300–450 K. In these compounds, the position of the IVCT band is at about

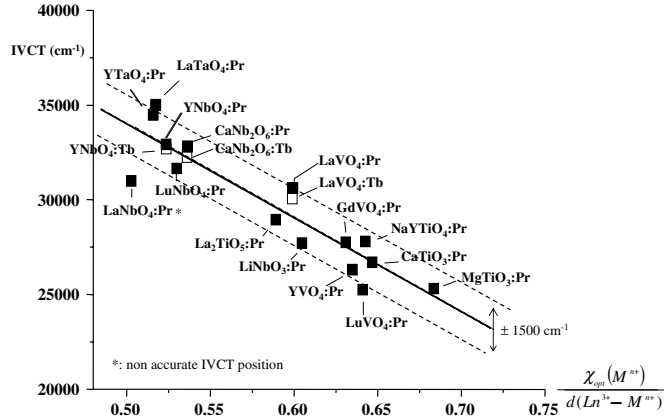

Figure 8. Variation of the IVCT band position against the ratio between the optical electronegativity of the closed-shell transition metal cation (M^{n+}) and the shortest interatomic distance between Ln^{3+} (Ln = Pr, Tb) and M^{n+}.

26 500 ± 200 cm^{-1} [2], and the energy barrier from $^1D_2$ to its crossover with the quenching state is in the range 3500–4000 cm^{-1} [8], i.e. significantly lower than in YNB ad CNB.

4. Discussion and conclusions

The analysis of the position of the IVCT band in a number of Pr^{3+}-doped closed-shell transition metal oxides has evidenced a linear dependence of the IVCT energy on the $\chi_{opt}(M^{n+})/d(Pr^{3+}-M^{n+})$ ratio, where $\chi_{opt}(M^{n+})$ is the optical electronegativity of the closed-shell transition metal ion M^{n+} and d (Pr^{3+}–M^{n+}) is the shortest interatomic distance between Pr^{3+} and M^{n+} [3]. As shown in figure 8, the experimental points are distributed along a straight line, whose equation can be easily determined by the least-square method:

$$\mathrm{IVCT}(Pr^{3+}, cm^{-1}) = 58\,800\text{–}49\,800\frac{\chi_{opt}(M^{n+})}{d(Pr^{3+}\text{–}M^{n+})}. \quad (2)$$

Even if not supported by a reliable physical model, this phenomenological equation is interesting because it allows one to predict the position of the IVCT band. This is important, since the relative intensity of the luminescence from the $^3P_0$ blue and $^1D_2$ red emitting level is, in fact, regulated by the position of the IVCT. Its effect can be formalized by considering the $R/(R+B)$ per cent intensity ratio (where R = red emission; B = blue emission) [2]. Its value is 100% when the energy of the IVCT band is lower than 28 000 cm^{-1}, as in the case of Pr^{3+}-doped titanates and vanadates in which $^1D_2$ is the only emitting level at room temperature. In contrast, IVCT bands located above 28 000 cm^{-1} cause only the partial quenching of the $^3P_0$ emission, with $R/(R+B) < 100\%$. This is the case for most of the niobate hosts that we have tested [3], including CNB and YNB which fit our phenomenological model quite well (see figure 8). We point out that, despite the existence of a number of exceptions, the accuracy of this model is of the order of ±1500 cm^{-1} (about 0.2 eV), surprisingly good if one considers the actual complexity of the problem. It is evident that at the present state of the research the availability of experimental data constitutes a crucial aspect. In this context, the investigation of Tb^{3+} luminescence in closed-shell transition metal oxides provides useful information. However, whereas the Tb^{3+} emission is completely quenched in a number of materials like vanadates and titanates as a consequence of the relative position of the $^5D_3$, $^5D_4$

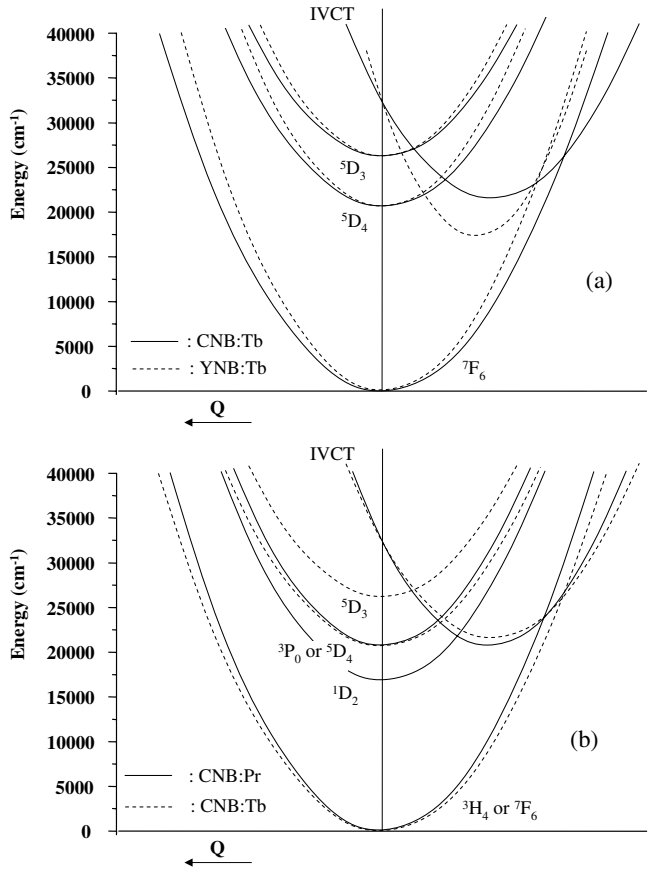

Figure 9. Single configurational coordinate diagrams for Tb^{3+} in $CaNb_2O_6$ and $YNbO_4$ (a) and for Pr^{3+} or Tb^{3+} in $CaNb_2O_6$ (b).

and IVCT states, it is detectable in the niobates, making them very suitable hosts for comparing the Pr^{3+} and Tb^{3+} luminescence properties. YNB and CNB are representative examples of this family, containing tetrahedrally and octahedrally coordinated niobate groups respectively, and having different emission properties. Nevertheless, we have observed in the room-temperature excitation spectra of figure 4 that the position of the IVCT band is in the same energy range within a few hundreds of cm^{-1}, independently of the Nb^{5+} coordination and of the optically active ion. Examining the spectra in more detail allowed us however to evidence a slight energy downshift of the IVCT position in the Tb^{3+}-doped niobates (see figure 8). A similar trend has also been observed in $LaVO_4$ crystals doped with Pr^{3+} or Tb^{3+} [16]. Using the IVCT energies at room temperature, the values of the activation energies to the crossover points determined in the previous section and considering the structural features of the compounds, we propose single configurational coordinate diagrams consistent with the observed excited-state dynamics. In figure 9(a) we compare the results obtained for Tb^{3+} in the two considered hosts; in figure 9(b) the schemes obtained for Pr^{3+} and Tb^{3+} in the same host, CNB, is reported.

For the sake of simplification, the energy of the IVCT state was taken at the average value of 32 500 cm^{-1} for all the compounds at room temperature and the energy levels $^5D_3$, $^5D_4 = {}^3P_0$ and $^1D_2$ were assumed to be 26 000, 20 500 and 16 500 cm^{-1} respectively. The

ground state ($^3H_4$ or $^7F_6$) was taken as the origin of energies. Considering the diagram in figure 9(b), it is clear that the relaxation mechanism occurring after excitation in the IVCT band is qualitatively similar for the two ions. Once the cross-relaxation processes can be excluded owing to the low doping level, the thermal quenching of the $^3P_0$ and $^5D_3$ levels is mostly driven by crossover to the IVCT state to feed the $^1D_2$ and $^5D_4$ levels, respectively. As $^5D_3$ is positioned higher in energy by $\approx$5500 cm^{-1} compared with $^3P_0$, the IVCT quenching is more efficient from the former than from the latter. Despite the fact that the IVCT bands lie in the same spectral range in the four niobates and the $^3P_0$ (Pr^{3+}) and $^5D_4$ (Tb^{3+}) levels have the same energy within a few tens of cm^{-1}, only the emission from the former is strongly quenched at room temperature, whereas that of the latter is not (see figure 1). This difference of behaviour is accounted for by considering the effects of the multiphonon relaxation from the $^3P_0$ to the $^1D_2$ next lower level (discussed before) and of the higher lying states of Pr^{3+} (mainly $^3P_1$ and $^1I_6$), that can be thermally populated from $^3P_0$ inducing an additional relaxation channel to the IVCT state. In contrast to the above situation, the $^5D_4$ (Tb^{3+}) level and also the $^1D_2$ (Pr^{3+}) level can be non-radiatively depopulated at the present doping level only through a process involving the thermal population of the IVCT state followed by relaxation to the ground state. Another remarkable aspect is related to the thermally activated host sensitization of the RE^{3+} in YNB and not in CNB. This difference in behaviour is clearly connected to the emission properties of the hosts. In fact the emission spectrum of YNB is significantly shifted to higher energy with respect to that of CNB (figure 2). With the temperature increasing, its thermal broadening results in a significant overlap with the IVCT excitation band that in turn relaxes to the Pr^{3+} or Tb^{3+} lowest emitting state. The participation of the IVCT state in the energy transfer processes represents an element of interest deserving further investigations.

Acknowledgment

The authors gratefully thank Marie Louise Clément (LMI) for her help in preparing the powder samples.

References

[1] Boutinaud P, Pinel E, Oubaha M, Mahiou R, Cavalli E and Bettinelli M 2006 *Opt. Mater.* **28** 9
[2] Boutinaud P, Mahiou R, Cavalli E and Bettinelli M 2006 *Chem. Phys. Lett.* **418** 185
[3] Boutinaud P, Mahiou R, Cavalli E and Bettinelli M 2007 *J. Lumin.* **122/123** 430
[4] Reut E G and Ryskin A I 1973 *Phys. Status Solidi* a **17** 47
[5] Blasse G and Bril A 1968 *J. Electrochem. Soc.* **115** 1067
[6] Su Q 1991 *Proc. 2nd Int. Conf. on Rare-Earth Development and Applications* vol 2, ed G Xu *et al* (Beijing: International Academic Publishers) p 765
[7] Dorenbos P 2004 *J. Lumin.* **108** 301
[8] Boutinaud P, Putaj P, Mahiou R, Cavalli E, Speghini A and Bettinelli M 2007 *Spectrosc. Lett.* **40** 1
[9] Weitzel H and Schröcke H 1980 *Z. Kristallogr.* **152** 69
[10] Cummings J P and Simonsen S H 1970 *Am. Mineral.* **55** 90
[11] Lee S K, Chang H, Han C-H, Kim H-J, Jang H G and Park H D 2001 *J. Solid State Chem.* **156** 267
[12] Blasse G and Bril A 1968 *Z. Phys. Chem.* **57** 187
[13] Struck C W and Fonger W H 1971 *J. Appl. Phys.* **42** 4515
[14] Jia W, Jia D, Rodriguez T, Evans D R, Meltzer R S and Yen W M 2006 *J. Lumin.* **119/120** 13
[15] De Mello Donega C, Meijerink A and Blasse G 1995 *J. Phys. Chem. Solids* **56** 673
[16] Krumpel A, Van der Kolk E, Dorenbos P, Boutinaud P, Cavalli E and Bettinelli M 2007 *J. Mater. Sci. Eng.* B at press doi:10.1016/j.mseb.2007.07.074